DYNAMIC FEM ANALYSIS OF MULTIPLE CMUT CELLS IN IMMERSION

Baris Bayram, Goksen G. Yaralioglu, Arif Sanli Ergun, Ömer Oralkan, and Butrus T. Khuri-Yakub
Edward L. Ginzton Laboratory, Stanford University, Stanford, CA 94305-4088

Abstract – **This paper reports on the accurate modeling of immersion capacitive micromachined ultrasonic transducers (cMUTs) using the time-domain, nonlinear finite element package, LS-DYNA, developed by Livermore Software Technology Corporation (LSTC). A capacitive micromachined ultrasonic transducer consists of many cMUT cells. In this paper, a square membrane was used as the unit cell to cover the transducer area by periodic replication on the surface. The silicon membrane, silicon oxide post and insulation layer were modeled, and the contact region was defined on the membrane and the substrate surfaces. The 3-D finite element model also included a 500 μm-thick substrate and the acoustic fluid medium, to take into account two main sources of coupling in cMUTs: Scholte wave propagating at the solid-fluid interface and Lamb wave propagating in the substrate. A highly efficient perfectly matched layer (PML) absorbing boundary condition was designed for the acoustic medium to truncate the computational domain. The cMUT was biased in-collapse or out-of-collapse with an applied potential difference between the membrane and substrate electrodes: a rectangular pulse excitation was then used for the conventional, collapsed or collapse-snapback operations of the cMUT. Collapsed operation of the cMUT generated six times greater acoustic output pressure (641 kPa) than the conventional operation (107 kPa) at both the same bias voltage (83 V) and the pulse amplitude (+5 V). The vacuum backing and impedance-matched backing were compared to determine the influence of wave reflections from the bottom of the substrate in the collapsed operation. The dynamic FEM results were compared to the experimental results for conventional and collapse-snapback operations by applying step voltages on biased cMUT membranes. The acoustic output pressure measurements of the cMUT were performed with a hydrophone. The hydrophone calibration data was used to find the sensed pressure. Taking the attenuation and diffraction losses into account, the pressure on the cMUT surface was extracted. The cMUT generated 348 kPa and 1040 kPa in the conventional and collapse-snapback operations, respectively, and good agreement was observed with the dynamic FEM results.**

I. INTRODUCTION

Capacitive micromachined ultrasonic transducers (cMUTs) emerged as an alternative to piezoelectric transducers in ultrasonic applications [1-4]. A new operation regime, collapsed operation, was proposed for the cMUTs [5]. Based on static FEM calculations, the collapsed operation provided coupling efficiency (k_T^2) greater than 0.7, when the cMUT was initially collapsed by applying a voltage higher than the collapse voltage, and then biased between the collapse and snapback voltages [5]. Experimental characterization of cMUTs operating in the collapsed regime verified the FEM calculations [6]. Recently, a new operation regime, collapse-snapback operation, was proposed to achieve high acoustic output pressure when the cMUT was operated in and out-of collapse [7]. The static and dynamic finite element calculations were in good agreement with the experimental measurements [7].

The design of cMUTs for collapsed and collapse-snapback operations required nonlinear finite element analysis, which included the contact dynamics. This paper presents our capability to perform fast and accurate FEA to design the cMUTs for both linear and nonlinear operations using LS-DYNA [8], which features an explicit solver and extended contact and material types to perform the crashworthiness analysis [9].

II. FINITE ELEMENT CALCULATIONS

Finite element methods (FEM) were used to analyze the cMUT using a commercially available FEM package (LS-DYNA 970) [8]. The FEM model of an immersed one-quarter of a square cMUT cell is shown in Fig. 1. Symmetry boundary conditions were applied to cover the transducer area by periodic replication (Fig. 1). The silicon membrane was supported on the edges with silicon oxide posts. There was a vacuum gap between the membrane and the substrate, which attracted each other, due to the applied voltages on the electrodes defined on the bottom of the membrane and on the top of the substrate with full coverage. The electrodes were assumed to be infinitesimally thin. A thin insulation layer of silicon oxide over the highly doped silicon substrate prevented shorting the ground and the membrane electrodes in collapse. Contact surfaces were defined on the bottom of the membrane and on the top of the insulation layer to model the collapse of the membrane. The 3-D finite element model also included a 500 μm-thick substrate and the acoustic fluid medium. A highly efficient perfectly matched layer (PML) absorbing boundary condition was designed for the acoustic medium to truncate the computational domain [10]. The physical dimensions of the cMUT used in the calculations are given in Table I.

TABLE I
PHYSICAL DIMENSIONS OF THE 2-D cMUT

Side length (L) (μm)	30
Membrane thickness (T) (μm)	1.2
Gap thickness (G) (μm)	0.18
Insulating layer thickness (I) (μm)	0.10
Cell periodicity (C) (μm)	35
Substrate (S) (μm)	500

0-7803-8412-1/04/$20.00 (c)2004 IEEE.

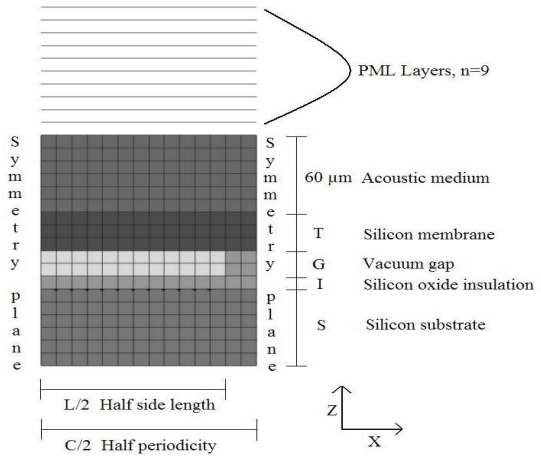

Figure 1. The cMUT simulation model

The center frequency of the unbiased membrane was 10 MHz in water. This cMUT design featured collapse and snapback voltages of 96 V and 70 V, respectively.

Prior to the dynamic analysis, the cMUT cell was statically biased at a voltage using the dynamic relaxation [9] within the intended operation regime. A pulse was subsequently applied to determine the acoustic output pressure.

III. RESULTS

The cMUT cell was biased at 83 V both in the conventional and in the collapsed operation regimes. Impedance-matched backing of the substrate was assumed in this calculation. A +5V, 20 ns pulse was then applied, and the acoustic output pressure, 60 µm away from the cMUT surface, was calculated (Fig. 2(a)). Conventional and collapsed operations generated 107 kPa and 641 kPa, respectively. The frequency spectrum of the pressure was corrected for the spectrum of the pulse (Fig. 2(c)). The center frequencies were 9.2 MHz (130% BW) in the conventional operation and 21.6 MHz (108% BW) in the collapsed operation. Then the pulse was increased to +30 V (Fig. 2(b)). Conventional and collapsed operations generated 770 kPa and 4260 kPa, respectively. The center frequencies were 8.6 MHz (132% BW) in the conventional operation and 22.7 MHz (84% BW) in the collapsed operation.

The impedance-matched backing of the substrate is compared to vacuum backing in Figs. 3(a,b). The cMUT was biased at 120 V in the collapsed operation and a -30 V rectangular pulse was applied for 20 ns. The vacuum backing caused substrate reflections at multiples of approximately 10 MHz, as was expected for 500 µm-thick substrate (Fig. 3(b)).

The physical parameters of the cMUT used in the experiments are listed in Table II. The active area of the cMUT is 64% of the total 1180-µm×280-µm transducer area, which consists of four 2-D cMUT elements connected together.

Transmit experiments were performed by measuring the pressure produced by the cMUT, using a calibrated hydrophone in the far field. The details of the experimental setup can be found

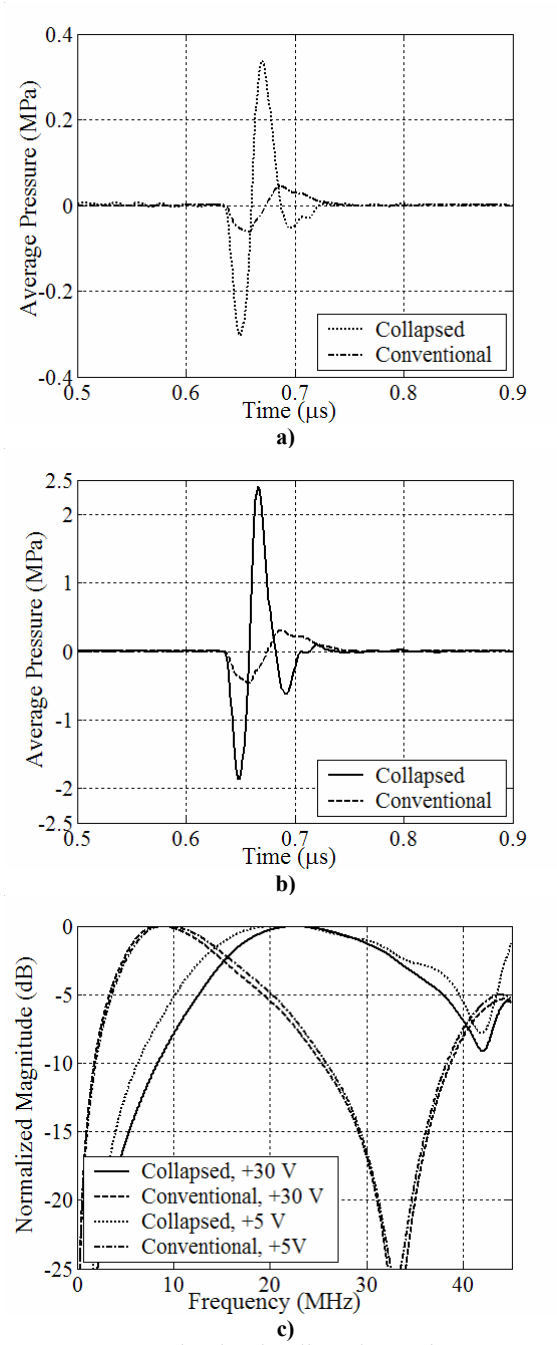

Figure 2. Conventional and Collapsed operations. V_{BIAS}=83 V. a) Average pressure. +5 V, 20 ns pulse. b) Average pressure. +30 V, 20 ns pulse. c) Normalized frequency spectrum of average pressure corrected for the spectrum of the pulse.

in [11]. The measured voltage signal by the hydrophone was processed in the frequency domain with the hydrophone calibration, the attenuation and the diffraction spectrums and inverse Fourier transform was used to determine the pressure at the cMUT surface as a function of time.

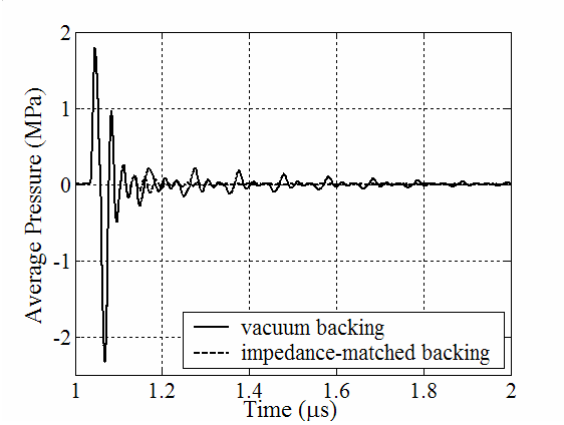

Figure 3. Substrate Backing Effect. V_{BIAS}=120 V. a) Average pressure. -30 V, 20 ns pulse. b) Normalized frequency spectrum of average pressure corrected for the spectrum of the pulse.

TABLE II
PHYSICAL PARAMETERS OF THE 2-D CMUT USED IN EXPERIMENTS

Length of the transducer, μm	1180
Width of the transducer, μm	280
Number of cells per element	4 x 52
Cell shape factor	Hexagon
Cell radius (r_{cell}), μm	16
Electrode radius (r_{el}), μm	8
Electrode thickness (t_{el}), μm	0.3
Membrane thickness (t_m), μm	1.06
Gap thickness (t_g), μm	0.22
Insulating layer thickness (t_i), μm	0.3
Silicon substrate thickness, μm	500
Collapse voltage, V	130
Snapback voltage, V	110

Average acoustic pressures on the cMUT surface are depicted in Fig. 4. The cMUT was biased at 50 V and excited by a +70 V pulse for t_P=1 μs for large signal conventional operation. In the rising edge of the pulse, peak-to-peak pressure of 0.18 MPa (2.5 kPa/V) was generated whereas the falling edge of the pulse resulted in 0.35 MPa (5 kPa/V) peak-to-peak pressure. The pulse was increased to +90 V for the collapse-snapback operation. In the collapsing cycle, peak-to-peak pressure of 0.23 MPa (2.5 kPa/V) was generated whereas the snapback cycle resulted in 1.04 MPa (11.5 kPa/V) peak-to-peak pressure. The acoustic output pressure per volt of 5 kPa/V in the conventional operation increased to 11.5 kPa/V in collapse-snapback operation when the snapback cycle was considered. The collapsing cycle generated 2.5 kPa/V in both conventional and collapse-snapback operations. The dynamic FEM results are depicted in Fig. 5, and good agreement between the FEM and experimental results is observed.

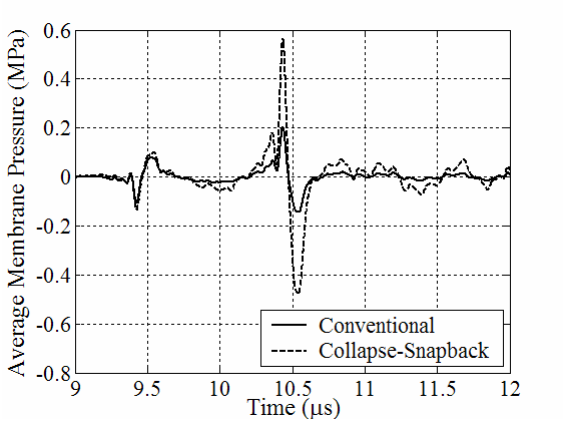

Figure 4. Experimental Results in Conventional and Collapse-Snapback operations. V_{BIAS}=50 V. +70 V, 1 μs unipolar pulse for conventional operation. +90 V, 1 μs unipolar pulse for collapse-snapback operation.

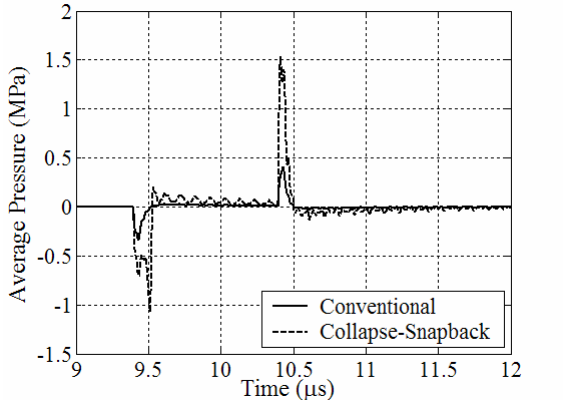

Figure 5. Dynamic FEM Results in Conventional and Collapse-Snapback operations. V_{BIAS}=50 V. +70 V, 1 μs unipolar pulse for conventional operation. +90 V, 1 μs unipolar pulse for collapse-snapback operation.

IV. DISCUSSION

Time domain finite element packages use either implicit or explicit time integration methods (LS-DYNA). Implicit methods result in unconditional stability in linear problems, and large time steps can be used in the calculations. However, implicit methods become unstable for highly nonlinear contact problems. Explicit methods are stable for even highly nonlinear situations, but the stability requires that very small time steps be used in each calculation. The time step is bounded by the largest natural frequency of the structure, which in turn is bounded by the highest frequency of any individual element in the finite element mesh [9]. The uncoupled equation sets in the explicit method allow a faster solution for each time step calculation, and the computation time scales almost linearly with the number of elements in the model. Implicit methods, due to the solution of the coupled equation sets, become impractical for large models. Therefore, explicit methods dominate the time domain, nonlinear analysis of very large models. We chose to use LS-DYNA in the finite element calculations, due to the availability of enhanced contact capabilities and explicit time domain solver.

The cMUT model is schematically depicted in Fig. 1. The dimensions are not drawn to scale, due to large aspect ratios in the model (0.1 μm insulation layer, 500 μm substrate). Fine spatial resolution in the meshing of the model usually increases the accuracy of the results. The average fluid and substrate mesh sizes were 1.25 μm and 2 μm, respectively. Higher spatial resolution increased the efficiency and the stability of the PML implementation [12]. The spacing between the neighboring absorbing layers was selected equal to the fluid mesh size. The anisotropic loss introduced in the PML increased smoothly from zero on the boundary to the maximum value on the outmost layer [13]. The gradual increase of the anisotropic loss reduced the reflections caused by passing from one layer to another, and significantly improved the absorption efficiency of the designed PML [12]. The additional computational cost of the PML was 80% of the finite element calculations performed without PML implementation. However, the presence of the PML reduced the fluid domain to 60 μm in the surface normal and provided faster calculation, compared to a larger model without absorbing boundary. The finite element calculations were performed up to 300,000 time steps successfully, and could be continued further.

An important difference between the experimental and simulation results was the following: the step response of the cMUT generated unipolar pressure (Fig. 5) in the simulations and bipolar pressure (Fig. 4) in the experiments. An assumption that was central in the calculations was the symmetry between each cell in the infinite transducer. This symmetry resulted in overdamped dynamic response. However, the cMUT used in the experiment had a finite size (1180-μm×280-μm). Therefore, the strictly enforced symmetry condition of the calculations was only weakly present, resulting in less damped response. A better understanding of this difference requires the finite element calculations of a finite size cMUT array (n×n cells, n~5).

V. CONCLUSION

We presented time-domain, coupled, nonlinear finite element calculations for an infinite cMUT using LS-DYNA. The finite element calculations were used to analyze the nonlinear operation regimes of the cMUT. Nonlinear operation regimes (collapsed and collapse-snapback) provided higher acoustic output pressures than the conventional operation. The finite element calculations were compared to the transmit experiment results performed with a hydrophone, and good agreement is observed.

ACKNOWLEDGMENT

This work is supported by ONR-NIH. The authors thank Mr. Can Bayram from Bilkent University for developing the ultrasonic field analysis tool using LABVIEW to control the main components of the experimental setup (the UNIDEX positioning system, voltage supplies, amplifier, and oscilloscope), Dr. Wayne L. Mindle from Livermore Software Technology Corporation (LSTC) for providing technical assistance in LS-DYNA and providing the object files for user-defined loading implementation, Dr. Khanh Bui from LSTC for providing useful information about the coupled-field analysis using LS-DYNA, and Dr. Morten Rikard Jensen from LSTC for providing technical support for full restart implementation in LS-DYNA.

REFERENCE

[1] M. I. Haller and B. T. Khuri-Yakub, "A Surface Micromachined Electrostatic Ultrasonic Air Transducer", in *Proceedings of Ultrasonics Symposium*, pp. 1241-1244, Cannes, France, 1994.

[2] H. T. Soh, I. Ladabaum, A. Atalar, C. F. Quate, and B. T. Khuri-Yakub, "Silicon Micromachined Ultrasonic Immersion Transducers", *Appl. Phys. Lett*., Vol. 69, pp. 3674-3676, Dec. 1996.

[3] P. C. Eccardt, K. Niederer, and B. Fischer, "Micromachined Transducers for Ultrasound Applications", in *Proceedings of Ultrasonics Symposium*, pp.1609-1618, 1997.

[4] I. Ladabaum, X. Jin, H. T. Soh, A. Atalar, B. T. Khuri-Yakub, "Surface Micromachined Capacitive Ultrasonic Transducers", *IEEE Trans. on UFFC*, Vol. 45, No. 3, pp. 678-690, May 1998.

[5] B. Bayram, E. Hæggström, G. G. Yaralioglu, and B. T. Khuri-Yakub, "A New Regime for Operating Capacitive Micromachined Ultrasonic Transducers", *IEEE Trans. on UFFC*, Vol. 50, No. 9, pp. 1184-1190, Sep 2003.

[6] Y. Huang, B. Bayram, A.S. Ergun, E. Hæggström, C.H. Cheng, and B.T. Khuri-Yakub, "Collapsed Region Operation of Capacitive Micromachined Ultrasonic Transducers based on Wafer-bonding Technique", in *Proceedings of IEEE Ultrasonics Symposium*, Vol. 2, pp. 1161-1164, 2003.

[7] B. Bayram, Ö. Oralkan, A.S. Ergun, E. Hæggström, G.G. Yaralioglu, and B.T. Khuri-Yakub, "Capacitive Micromachined Ultrasonic Transducer Design for High Power Transmission", accepted for publication in *IEEE Trans. on UFFC*.

[8] LS-DYNA 970, Livermore Software Technology Corporation, Livermore, CA 94551.

[9] LS-DYNA 970 Keyword User's Manual, Livermore Software Technology Corporation, Livermore, CA, 2003

[10] J. P. Berenger, "A Perfectly Matched Layer for the Absorption of Electromagnetic Waves", J. Comput. Phys., vol. 114, pp. 185-200, October 1994.

[11] O. Oralkan, X. Jin, F.L. Degertekin, and B.T. Khuri-Yakub, "Simulation and Experimental Characterization of a 2-D Capacitive Micromachined Ultrasonic Transducer Array Element," *IEEE Trans. on UFFC*, Vol. 46, No. 6, pp. 1337-1340, November 1999.

[12] G. Festa, and S. Nielsen, "PML Absorbing Boundaries", Bulletin of the Seismological Society of America, Vol. 93, No. 2, pp. 891-903, April 2003.

[13] X. Yuan, D. Borup, J.W. Wiskin, M. Berggren, R. Eidens, and S.A. Johnson, "Formulation and Validation of Berenger's PML Absorbing Boundary for the FDTD Simulation of Acoustic Scattering", *IEEE Trans. on UFFC*, Vol. 44, No. 4, pp. 816-821, July 1997.